Experimental determination of the conduction-band offset at GaAs/$Ga_{1-x}Al_xAs$ heterojunctions with the use of ballistic electrons

T. Forchhammer and E. Veje
Oersted Laboratory, Niels Bohr Institute, Universitetsparken 5, DK-2100 Copenhagen, Denmark

P. Tidemand-Petersson
Tele Danmark Research, Lyngsø Allé 2, DK-2970 Hørsholm, Denmark
(Received 24 March 1995; revised manuscript received 8 August 1995)

The conduction-band offset ΔE_c at GaAs/$Ga_{1-x}Al_xAs$ heterojunctions has been measured by observing radiative recombination of electrons, injected ballistically from $Ga_{1-x}Al_xAs$ into GaAs, with acceptors in GaAs. Additionally, the total band-gap energy difference ΔE_g between $Ga_{1-x}Al_xAs$ and GaAs was measured with the use of photoluminescence, permitting a determination of the conduction-band offset coefficient $Q_c \equiv \Delta E_c / \Delta E_g$. The measurements were carried out for various values of the mole fraction x of aluminum in the $Ga_{1-x}Al_xAs$ alloy, up to $x=0.53$. In the direct band-gap region (i.e., $x<0.39$), Q_c is constant and equal to 0.69. Above $x=0.39$, Q_c decreases steadily with increasing x.

I. INTRODUCTION

The conduction-band offset ΔE_c at a chemically abrupt heterojunction between two semiconductor materials is defined as the discontinuity in the conduction-band edges at the interface, and the conduction-band offset coefficient Q_c is defined as

$$Q_c \equiv \frac{\Delta E_c}{\Delta E_g} , \tag{1}$$

where ΔE_g is the difference between the bulk band-gap energies of the two materials forming the heterojunction. Correspondingly, the valence-band offset ΔE_v is the valence-band discontinuity, and the valence-band-offset coefficient Q_v is defined as

$$Q_v \equiv \frac{\Delta E_v}{\Delta E_g} .$$

These quantities are of fundamental interest in basic research, and, furthermore, they are crucial input parameters for the design of heterostructure devices; see, for example, Ref. 1. Unfortunately, band offsets have been notoriously difficult to determine experimentally and also to predict theoretically to the needed accuracy,[2] which for applications is comparable to the temperature at which the device will have to operate, i.e., a few meV at low temperatures. Widely used measurements have been based on electrical as well as optical methods (see, e.g., the first 25 references cited in Ref. 3), and evidently a wide range of band-offset values has been reported with no apparent correlation among the sample preparation or the measurement method employed.[3] For example, Q_c values reported for GaAs/$Ga_{1-x}Al_xAs$ range between 0.5 and 0.88 (see, e.g., Fig. 7 in Ref. 4), but whether such a scattering reflects a possible dependence upon the mole fraction x, or sample production and preparation, or ambiguities in measurement procedures employed, is not clear at the moment.

Concerning optical methods, a popular one has been to measure the optical interband transition energies in quantum wells or superlattices, and to extract band-offset values by adjusting transition energies calculated from the well shape to experimental data. This method, however, requires precise knowledge about the spatial variation of the band structure of the sample, as discussed in detail in Ref. 3, and this may limit the precision of such measurements. Correspondingly for electrical measurements, the reliability of the band-offset determination by the capacitance-voltage (C-V) method depends on the concentration of traps near the interface, and a low trap concentration is required for a precise determination.[5]

In the present investigation, the experimental method used is of a direct nature. It is based on electroluminescence, and the basic principle is sketched in Fig. 1, in which band bendings at the heterojunction and also possible phonon-related processes have been omitted on purpose. Such details are crucial in the data reduction, and therefore they are included and discussed at length with references to our experimental findings concerning them in Sec. III. For a qualitative description of the fundamental processes involved in our experiments, they are, however, omitted here for clarity. In Fig. 1, due to an electric potential drop caused by an external source across the sample, electrons are injected ballistically from the n-type $Ga_{1-x}Al_xAs$ section (left) into p-type GaAs (right), where they may recombine radiatively with neutral acceptors. Evidently, in this picture

$$\Delta E_c = E_{h\nu} - E_{\mathrm{GaAs}} + E_A , \tag{2}$$

where $E_{h\nu}$ is the energy of photons emitted from radiative recombination processes, E_{GaAs} is the band-gap energy of GaAs, and E_A is the acceptor energy in GaAs. Thus the conduction-band offset can be determined with the use of electroluminescence, by observing and identifying the photon emission which results from the appropri-

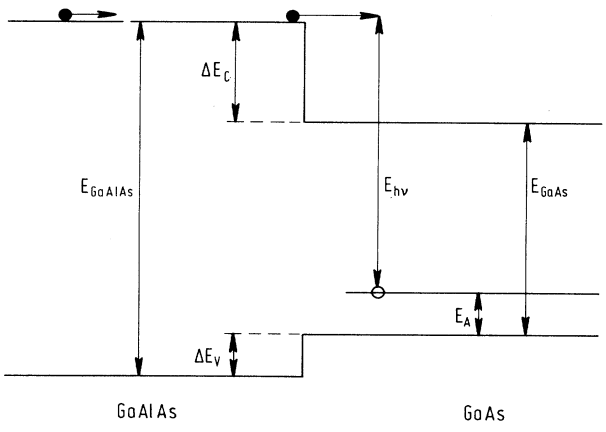

FIG. 1. A schematic diagram of the conduction- and valence-band edges at a GaAs/$Ga_{1-x}Al_xAs$ heterojunction, ignoring band bending. E_{GaAs} and $E_{Ga_{1-x}Al_xAs}$ are the band-gap energies in GaAs and $Ga_{1-x}Al_xAs$, respectively. ΔE_c is the conduction-band offset, ΔE_v is the valence-band offset, and E_A is the acceptor level in GaAs. $E_{h\nu}$ is the energy of photons emitted when ballistic electrons emitted from $Ga_{1-x}Al_xAs$ recombine with neutral acceptors in GaAs.

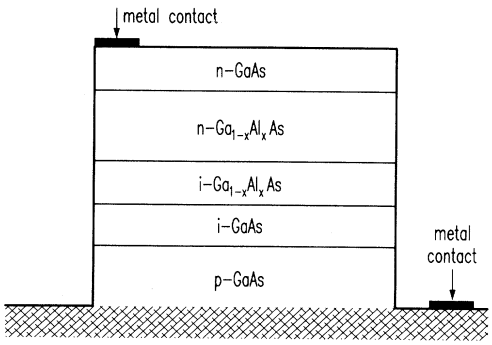

FIG. 2. A schematic cross section of a GaAs/$Ga_{1-x}Al_xAs$ p-i-n heterodiode. The relative layer thicknesses are not drawn to scale.

ate radiative recombination sketched in Fig. 1.

The experimental technique outlined above has previously[6,7] been used to determine the conduction-band offset for GaAs/$Ga_{1-x}Al_xAs$ heterojunctions for mole fractions x between 0.2 and 0.4. The purpose of the present work has been twofold, namely to check the results presented in Refs. 6 and 7, and also to extend the measurements to smaller and larger mole fractions.

II. EXPERIMENTAL PROCEDURE

The heterostructures used here were grown by molecular-beam epitaxy (MBE) in a VARIAN Modular GEN II growth chamber. In each case, first a 2-μm-thick GaAs buffer, p-type doped with beryllium (5×10^{23} atoms per m^3), was grown on a semi-insulating GaAs wafer. The buffer was terminated with a 10-nm-thick undoped GaAs layer. On top of the buffer a 0.2-μm-thick undoped $Ga_{1-x}Al_xAs$ spacer was grown, followed by a 0.8-μm-thick $Ga_{1-x}Al_xAs$ layer of same mole fraction and doped with 2×10^{23} silicon atoms per m^3 (n type). Finally, the structure was capped with a 10-nm-thick layer of GaAs, also doped with 2×10^{23} silicon atoms per m^3. The different layers were so thick that their energy-band structures can be regarded as being bulk structures, unmodified by spatial confinements.

After growth, p-i-n heterodiodes were formed by etching through the layer of $Ga_{1-x}Al_xAs$ on part of the sample and subsequently evaporating gold contacts on small sections of the unetched surface as well as the uncovered GaAs buffer. A schematic cross section of such a diode is shown in Fig. 2.

The diodes were mounted strain free in a closed-cycle helium refrigeration system which was capable of cooling the samples to 10 K. Measurements were made by applying an electric potential drop across the diodes in the forward direction and measuring the resultant electroluminescence. Most of the data reported here were taken with a sample temperature of 10 K, but in some cases additional measurements were carried out at slightly higher temperatures (always below 20 K) to increase the current through the diode and thus the electroluminescence signal, without increasing the electric potential drop across the sample.

Electroluminescence from the diodes was analyzed in a 1-m scanning spectrometer (McPherson model 2051) and detected with a photomultiplier (Hamamatsu model R 943-02) using single-photon counting.

The aluminum mole fraction x in $Ga_{1-x}Al_xAs$ was determined after growth with x-ray diffraction as described in Ref. 8. In addition, x was also determined from reflection high-energy electron-diffraction (RHEED) oscillations observed during MBE growth on special stationary wafers. This was carried out immediately before the samples of interest were grown on rotating wafers. The mole fractions determined with x-ray diffraction were from 6% to 15% larger than the corresponding data deduced from the RHEED measurements. The mole fraction values given below are only those determined with x-ray diffraction, because these measurements were carried out on samples cut from the same wafers that the diodes were made from, and also because of the small overall uncertainty and presumably lack of systematic errors related to the x-ray-diffraction measurements. The problem associated with determining the aluminum mole fraction has recently been discussed in detail; see the appendix in Ref. 9.

The band-gap energies of the different samples, and also the acceptor level in GaAs, were determined with photoluminescence, as described in Ref. 8. The band-gap energy of $Ga_{1-x}Al_xAs$ as a function of x found here is in close agreement with that reported in Ref. 8, yielding confidence in the reproducibility of the method.

III. DATA REDUCTION AND RESULTS

When band bending is included to the crude picture described in Sec. I (cf. Fig. 1), a potential barrier is added to the conduction band, on the $Ga_{1-x}Al_xAs$ side of the interface, and there will be a small potential well on the GaAs side. In Fig. 3 these modifications are incorporated, and all relevant quantities are specified. E_{DB} denotes the depletion barrier in $Ga_{1-x}Al_xAs$, and E_1 is a corresponding (but numerically smaller) downward band bending in GaAs. E_p is the photon energy at the intensity maximum in the electroluminescence (EL) spectrum, E_0 is an offset due to tunneling of electrons through the barrier E_{DB}, and E_A is the acceptor energy in GaAs. Superimposed on this, there will be an electric potential drop due to the forward external bias, which will cause conduction electrons to move from left to right, and valence-band holes from right to left in Fig. 3. The external bias will shift the band bendings back toward the flat-band condition shown in Fig. 1 (Ref. 7).

From Fig. 3, evidently

$$\Delta E_c = E_p + E_0 + E_1 - (E_{GaAs} - E_A) , \tag{3}$$

which substitutes Eq. (2).

In Fig. 3 is also sketched EL involving phonon emission. Equation (3) can equally well be applied to phonon replicas by correcting the energy of the replica with the well-established phonon energy of 36 meV for GaAs.

In the following, we first present two EL spectra. Then we describe how the five quantities in Eq. (3) were determined and also how the uncertainties related to them were estimated.

Figures 4 and 5 show the interesting sections of typical EL spectra from *p-i-n* diodes with mole fractions of 0.21 and 0.30, respectively. Typically, at shorter wavelengths, we observed the near-band-gap radiation of $Ga_{1-x}Al_xAs$, which can readily be identified.[9] At longer wavelengths we observed the corresponding near-band-gap radiation of GaAs, and in between these features the radiative recombination of ballistic electrons from the $Ga_{1-x}Al_xAs$ layer with acceptors in the GaAs layer appeared. In many cases, this radiation was much weaker than the near-band-gap emission from GaAs, the latter extending a long tail into the spectral region of interest concerning the phonon replicas. However, by using appropriate absorption filters, the region of interest could

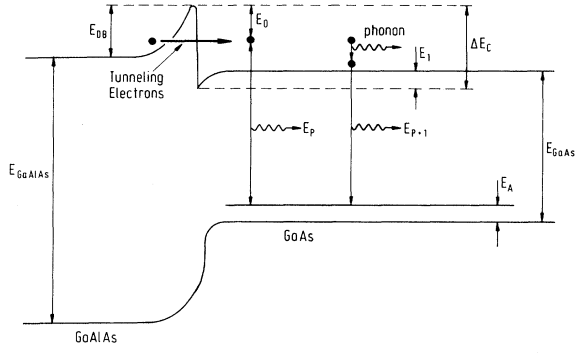

FIG. 3. Diagram of the conduction- and valence-band edges at a $GaAs/Ga_{1-x}Al_xAs$ heterojunction, including band bending. The diagram is not drawn to scale. The relative magnitudes of E_{DB} and E_1 are exaggerated to make these quantities visible.

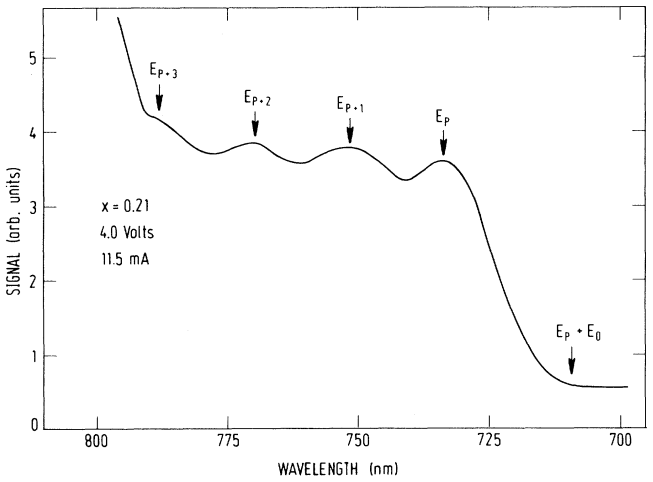

FIG. 4. Electroluminescence spectrum from a $GaAs/Ga_{1-x}Al_xAs$ heterodiode with $x=0.21$. The peak marked E_p results from radiative recombination of electrons emitted ballistically from $Ga_{1-x}Al_xAs$ with neutral acceptors in GaAs, cf. Figs. 1 and 3. The peaks marked E_{p+1}, E_{p+2}, etc. are phonon replicas. The wavelength corresponding to E_p+E_0 is marked with E_p+E_0.

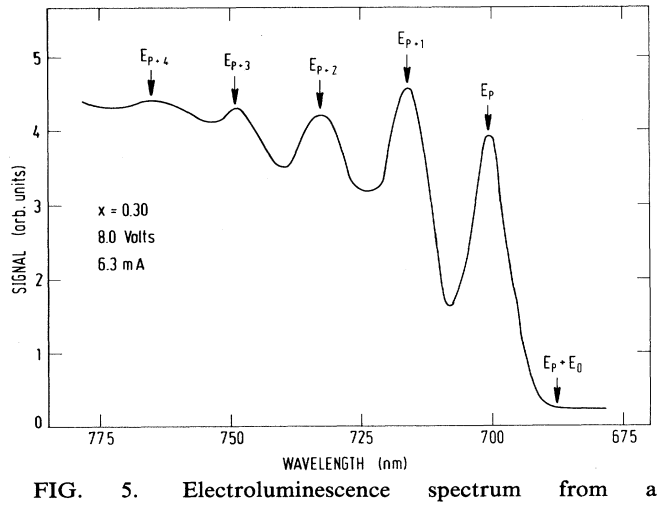

FIG. 5. Electroluminescence spectrum from a $GaAs/Ga_{1-x}Al_xAs$ heterodiode with $x=0.30$. The peak marked E_p results from radiative recombination of electrons emitted ballistically from $Ga_{1-x}Al_xAs$ with neutral acceptors in GaAs, cf. Figs. 1 and 3. The peaks marked E_{p+1}, E_{p+2}, etc. are phonon replicas. The wavelength corresponding to E_p+E_0 is marked with E_p+E_0.

be cleared satisfyingly well, as can be seen in Figs. 4 and 5.

The EL spectra were analyzed to determine the wavelength of the recombination peak, yielding E_p, and also the phonon replicas. These spectral features are marked E_p and $E_{p+1}, E_{p+2}, \ldots$, respectively, in Figs. 4 and 5.

In Figs. 4 and 5 the instrumental resolution of the optical spectrometer was 1.5 nm. The overall spectral resolution, as seen in Figs. 4 and 5, was set by the samples and not by the spectrometer. The largest component of the total linewidth is introduced by electron injection from $Ga_{1-x}Al_xAs$ to GaAs, because this is governed by tunneling through the barrier E_{DB}; see Ref. 6.

The resulting EL spectrum will be characterized by the tunneling current through the barrier. The current density, as a function of the electron energy, will have a maximum corresponding to a location between the bottom of the conduction band in $Ga_{1-x}Al_xAs$ and the top of the barrier. This is because the current density is the product of the Fermi distribution, which is steadily decreasing, and the tunneling probability which increases steadily with increasing energy; for details, see Ref. 6.

From Fig. 3 it can be seen that of all quantities in Eq. (3), E_p is the largest. Also, from Figs. 4 and 5 it can be seen that E_p can be determined with a relatively small uncertainty ($\approx 0.3\%$ or below). The substantially smaller quantity E_0 is somewhat more difficult to determine. It can be estimated satisfyingly well by calculating the tunneling current density as a function of the total electron kinetic energy and matching it self-consistently to the measured current density as outlined in Ref. 6. Although the uncertainty related to such a deduction of E_0 is relatively large; as compared to E_0, the method is satisfyingly good, because E_0 is a small quantity. In practice, it came out empirically that the tunnel current tends to zero at a kinetic energy close to E_{DB} (cf. Fig. 4 in Ref. 6), implying that the EL signal tends to the background level at a photon energy approximately equal to E_p+E_0; see Figs. 4 and 5, in which the wavelengths corresponding to E_p+E_0 have been marked with arrows.

The tunneling current and thus the photon energies of interest depend on the applied electric potential drop across the diode. To eliminate this effect, EL spectra were recorded for different voltages for each sample, and the data were extrapolated to zero potential drop. An example of such an extrapolation, for $x=0.30$, is given in Fig. 6. In this figure are shown values for E_p+E_0 as well as for E_p. As seen from Fig. 6, omission of such extrapolations to zero potential will introduce systematic errors, which albeit small cannot be neglected. Such extrapolations were not mentioned in Refs. 6 and 7.

Concerning E_1, electrons can be bound in the potential well related to E_1, and radiative recombination between such electrons and valence-band holes in the GaAs can be observed in photoluminescence (PL) studies.[10] Such radiative recombination is denoted the H band, and when present it can well be comparable in intensity to the ordinary PL spectral features.[10] It comes out that for same doping levels, the position of the H band, and thus the magnitude of E_1, depends little on the mole fraction x

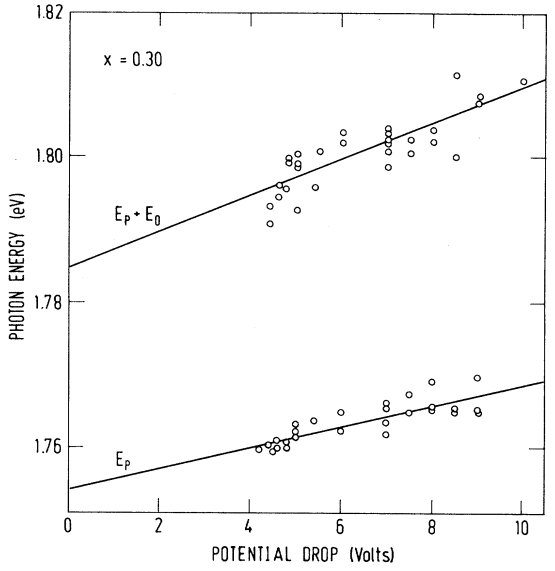

FIG. 6. The values of E_p and E_p+E_0 obtained with a heterodiode with Al mole fraction $x=0.30$, plotted vs the electric potential drop across the diode. The uncertainty associated with the extrapolations to zero potential drop are 5 meV for E_p and 8 meV for E_p+E_0.

(Ref. 10). For weakly doped samples, such as ours, E_1 can be so small that only very few electrons are trapped in the well, and, consequently, the H band is not seen in PL. In addition, in our samples, the nominally intrinsic layer of $Ga_{1-x}Al_xAs$ (cf. Fig. 2) included will reduce this band bending in the GaAs (cf. Ref. 7). In our PL measurements, a careful search was carried out for observing the H band, but the result was negative for all samples, indicating a high degree of flatness of the GaAs band edges. This is in agreement with the theoretical considerations presented in Ref. 11. By combining the theoretical data of Ref. 11 and the experimental results in Ref. 10 with the reduction in band bending due to the nominally intrinsic layer of $Ga_{1-x}Al_xAs$ as well as due to the external bias,[7] we have estimated E_1 to be from 3 to 5 meV. We have used a constant value of 4 meV, which is of sufficient accuracy, because E_1 is by far the smallest quantity in Eq. (3). No value for E_1 was listed in Refs. 6 and 7. The uncertainty we relate to E_1 is 2 meV. This amount has been included in the evaluation of the overall uncertainty, which confirmed that although our estimation of E_1 is somewhat arbitrary, it is clearly sufficiently good. In addition, if in the future a better determination of E_1 becomes available, all information necessary to carry out a correction of our final results is presented here.

Concerning the last two terms in Eq. (3), they can readily be derived from the PL spectra as well as the EL spectra. Both methods yielded $E_{GaAs}-E_A=1.492$ eV ± 0.001 eV.

The resulting values of ΔE_c and ΔE_v are given in Table I, in which the mole fractions obtained from x-ray

TABLE I. The first column gives the mole fraction x of the five samples investigated. The next two columns list the conduction-band offset ΔE_c and the valence-band offset ΔE_v, respectively. The fourth column shows the overall uncertainty related to ΔE_c or ΔE_v, as described in the text. Note, however, that ΔE_c and ΔE_v are related, because their sum equals the difference in band-gap energies between $Ga_{1-x}Al_xAs$ and GaAs, which has a total uncertainty of only 2 meV, because the band-gap energies have been determined with PL. The two last columns present our results for the conduction-band-offset coefficient $Q_c \equiv \Delta E_c / \Delta E_g$, and the overall uncertainties related to Q_c.

Mole fraction, x	ΔE_c (meV)	ΔE_v (meV)	ΔE (meV)	Q_c	ΔQ_c
0.11	106	46	16	0.70	0.11
0.21	213	84	14	0.72	0.05
0.30	289	128	11	0.69	0.03
0.42	359	208	18	0.63	0.03
0.53	342	251	19	0.58	0.03

diffraction are also included. The overall uncertainty in each extrapolation to zero bias was evaluated, and the resulting uncertainties are also included in Table I. Extrapolations of the energies related to the photon replicas yielded results in agreement with the data in Table I. However, since data derived from the phonon replicas generally have larger uncertainties, they have not been included in the final results.

As discussed in detail in Ref. 7, the validity of the above-described data reduction, and thus the results, hinges on the quality of the p-n heterodiodes used, because noticeable diffusion of Be from GaAs to $Ga_{1-x}Al_xAs$ would result in a vanishing or even negative value for E_{DB}. The samples used here were grown at a relatively low substrate temperature, to avoid diffusion of Be. Previous work with δ-doped GaAs has indicated that, although the crystal quality of GaAs is not as good as if it had been grown at a higher temperature, it is in this way possible to control spatially the doping with Be sufficiently well. Furthermore, if appreciable amounts of Be had diffused into the $Ga_{1-x}Al_xAs$, this would have been observed in the PL spectra. Previous work with silicon-doped $Ga_{1-x}Al_xAs$/GaAs structures has shown that doping with Si as done here results in a slightly n-type $Ga_{1-x}Al_xAs$ close to the interface. For all samples, I-V characteristics indicated that the diodes were of high quality.

IV. DISCUSSION

In Fig. 7 are plotted our values for ΔE_c (upper section) and ΔE_v (lower section) versus the mole fraction x. Whereas ΔE_v decreases steadily and almost in proportion to x, there is clearly a turnover for ΔE_c. This is in close agreement with the crossover between the direct (Γ) band gap for low values of x and the indirect (X) band gap for high values of x. The crossing point is now well

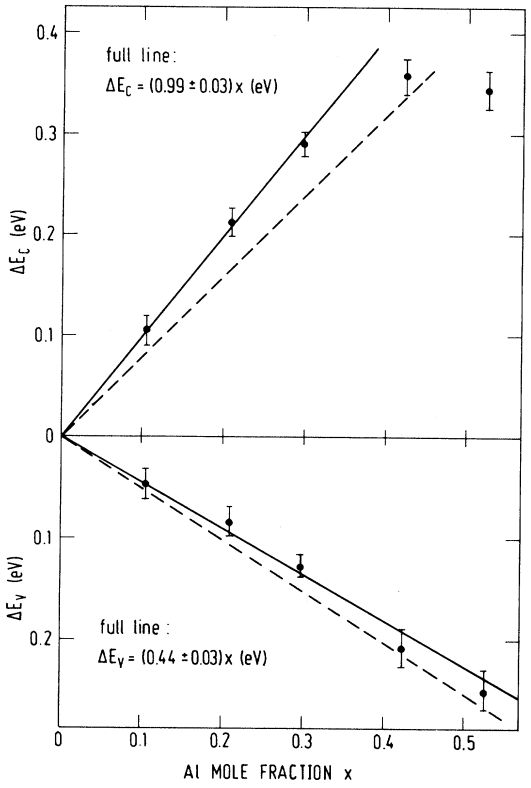

FIG. 7. In the upper section of the figure the conduction-band offset ΔE_c is plotted vs the Al mole fraction x. Corresponding data for the valence-band offset are plotted in the lower section of the figure. Straight-line fits to the data are shown with full-drawn lines, and the results presented in Ref. 13 are given with dashed lines.

established to occur for $x = 0.385$ (Ref. 12; for a detailed discussion, see Ref. 9). In Fig. 7 the full-drawn lines show linear fits to our results for ΔE_v and for ΔE_c below $x = 0.38$. Clearly, our data for $x = 0.42$ and 0.53 fall below the extrapolation of the latter line, and a line drawn through these two points will cross the full-drawn line in Fig. 7 at $x = 0.37$, lending support to our results.

Conduction- and valence-band-offset data for GaAs/$Ga_{1-x}Al_xAs$ interfaces published before 1992 have been compiled by Missous.[13] From the data available at that time, Missous concluded that $\Delta E_v = (0.51 \pm 0.04)x$ eV for $0 \le x \le 1$, and $\Delta E_c = (0.80 \pm 0.03)x$ eV for $0 \le x < 0.45$. For $x > 0.45$, ΔE_c decreases steadily. These relations for ΔE_v and ΔE_c are shown with dashed straight lines in Fig. 7.

Concerning ΔE_v, the best linear fit to our data (shown with full-drawn line) is $\Delta E_v = (0.44 \pm 0.03)x$ eV, which within uncertainty limits agrees with the Missous fit given above. However, all of our data fall above the dashed line.

Concerning ΔE_c (upper section in Fig. 7), our results below $x = 0.38$ fall clearly above the dashed line reproduced from Ref. 13. Based upon the facts that our values

for ΔE_v agree satisfyingly well with Ref. 13, and also that our total band-gap energies are in close agreement with recently published data of high quality (see Ref. 8 and references therein), we conclude that the relation $\Delta E_c = (0.80 \pm 0.03)x$ eV published in Ref. 13 underestimates ΔE_c. The linear fit we find (full line in Fig. 8), is $\Delta E_c = (0.99 \pm 0.03)x$ eV. The difference between the present investigation and Ref. 13 is traceable to the following two points. Measurements prior to 1992 seem to underestimate the total band-gap energy, and also to locate the crossover between direct and indirect band gap to $x = 0.45$ instead of $x = 0.385$.

In Fig. 8 are plotted the values for Q_c listed in Table I, versus x. In this figure are also included data given in Refs. 6, 7, 14, and 15. We note satisfyingly good agreements with Refs. 6 and 7, which were based on the same method as used here; with Ref. 14, based on internal photoemission; and also with Ref. 15, based on C-V and I-V measurements.

As discussed above, in the direct band-gap region (i.e., $x < 0.385$) both ΔE_c and ΔE_v are proportional to x (cf. the two full lines in Fig. 7). Thus, in this region, Q_c is independent of x, and from the slopes of the two full-drawn lines in Fig. 7, $Q_c = 0.69$, indicated with a straight horizontal line in Fig. 8. Note that all three of our data points in this region fall slightly above this line (their average value being 0.70), because the proportionality between ΔE_v and x, as taken from Fig. 7, is determined from all five points in the lower section of Fig. 7. The points for $x = 0.42$ and 0.53 fall relatively low, yielding a slightly larger constant of proportionality than if these results had been omitted. The data from Refs. 6, 7, and 14 might indicate a slight decrease in Q_c for increasing x, below $x = 0.385$, but such a variation in Q_c is not in accordance with the proportionalities depicted in Fig. 7. A variation in Q_c in this interval would imply deviation from proportionality between x and either (or both) ΔE_v or ΔE_c. From the data given in Ref. 13, one arrives at the value $Q_c = 0.61$, which is shown with the dashed line in Fig. 8. The lower value is related to the smaller ΔE_c, as discussed above.

For $x > 0.385$, Q_c decreases with increasing x. Since ΔE_v increases steadily and ΔE_c decreases with increasing x (cf. Fig. 7), Q_c will decrease steadily in the interval $0.385 < x < 1$.

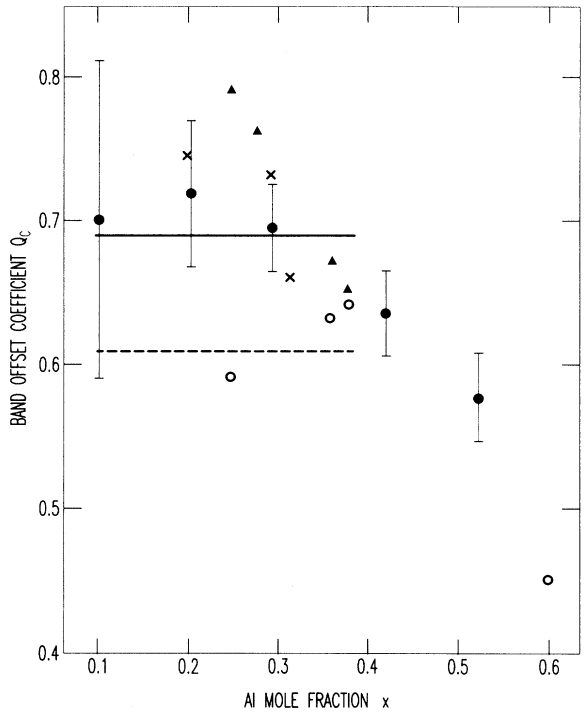

FIG. 8. The conduction-band-offset coefficient $Q_c \equiv \Delta E_c / \Delta E_v$ plotted vs the Al mole fraction x. ●: this work; x: data from Refs. 6 and 7; ▲: Ref. 14; ○: Ref. 15. The full-drawn line shows the ratio of the slopes of the two full-drawn lines in Fig. 7, and the dashed line results from data in Ref. 11.

ACKNOWLEDGMENTS

This work has been supported by the Danish Natural Science Research Council, the Danish National Agency of Technology, the Carlsberg Foundation, Director Ib Henriksens Foundation, and the NOVO Nordic Foundation. All grants are highly appreciated.

[1] *Heterojunction Band Discontinuities; Physics and Device Applications,* edited by F. Capasso and G. Margaritondo (Elsevier Science, Amsterdam, 1987).
[2] M. S. Hybertsen, Mater. Sci. Eng. B **14**, 254 (1992).
[3] R. F. Kopf, M. H. Herman, M. L. Schnoes, A. P. Perley, G. Livescu, and M. Ohring, J. Appl. Phys. **71**, 5004 (1992).
[4] H. Heinrich and J. M. Langer, in *Festkörperprobleme XXVI (1986) Advances in Solid State Physics,* edited by P. Grosse (Vieweg, Braunschweig, 1986), Vol. 26, p. 251.
[5] H. Okumura, S. Misawa, and S. Yoshida, Surf. Sci. **174**, 324 (1986).
[6] C. L. Petersen, M. R. Frei, and S. A. Lyon, Phys. Rev. Lett. **63**, 2849 (1989).
[7] S. A. Lyon and C. L. Petersen, Semicond. Sci. Technol. **7**, B21 (1992).
[8] M. El Allali, C. B. Sørensen, E. Veje, and P. Tidemand-Petersson, Phys. Rev. B **48**, 4398 (1993).
[9] L. Pavesi and M. Guzzi, J. Appl. Phys. **75**, 4779 (1994).
[10] Y. R. Yuan, M. A. A. Pudensi, G. A. Vawter, and J. L. Merz, J. Appl. Phys. **58**, 397 (1985).
[11] I. Balslev, Semicond. Sci. Technol. **2**, 437 (1987).
[12] M. Guzzi, E. Grilli, S. Oggioni, J. L. Staehli, C. Bosio, and L. Pavesi, Phys. Rev. B **45**, 10 951 (1992).
[13] M. Missous, in *Properties of Aluminum Gallium Arsenide,* edited by S. Adachi, EMIS Datareview Series No. 7 (INSPEC, London, 1993), p. 73.
[14] K. W. Goossen, S. A. Lyon, and K. Alavi, Phys. Rev. B **36**, 9370 (1987).
[15] J. Batey and S. L. Wright, J. Appl. Phys. **59**, 200 (1986).